

# Imaging Features following Thermal Ablation of Lung Malignancies

Sophie Chheang, MD<sup>1</sup> Feredoin Abtin, MD<sup>2</sup> Antonio Guteirrez, MD<sup>2</sup> Scott Genshaft, MD<sup>2</sup>  
Robert Suh, MD<sup>2</sup>

<sup>1</sup> Division of Interventional Radiology, Department of Radiology, Weill Cornell Medical College, New York-Presbyterian Hospital, New York, New York

<sup>2</sup> Thoracic Imaging Section, Department of Radiological Sciences, David Geffen School of Medicine at UCLA, Los Angeles, California

**Address for correspondence** Robert Suh, MD, Thoracic Imaging Section, Department of Radiological Sciences, David Geffen School of Medicine at UCLA, 757 Westwood Plaza, Suite 1621, Los Angeles, CA 90095-7437 (e-mail: rsuh@mednet.ucla.edu).

Semin Intervent Radiol 2013;30:157–168

## Abstract

### Keywords

- ▶ lung cancer
- ▶ thermal ablation
- ▶ imaging findings
- ▶ positron emission tomography
- ▶ computed tomography
- ▶ radiofrequency
- ▶ microwave
- ▶ cryotherapy

Percutaneous image-guided thermal ablation is gaining attraction as an effective alternative to surgical resection for patients with primary and secondary malignancies of the lung. Currently, no standard follow-up imaging protocol has been established or uniformly accepted. The early identification of residual or recurrent tumor would in theory enable the practitioner to offer expeditious retreatment or alternative treatment. This review elaborates on the imaging findings following thermal ablation, both heat- and cold-based, of nonresectable pulmonary malignancies.

**Objectives:** Upon completion of this article, the reader will be able to discuss the imaging findings following thermal ablation, highlight the potential imaging pitfalls, and discuss the relative merits of contrast enhancement and fluorodeoxyglucose uptake in differentiating malignancy from inflammatory or infectious processes in the postablation period.

**Accreditation:** This activity has been planned and implemented in accordance with the Essential Areas and policies of the Accreditation Council for Continuing Medical Education through the joint sponsorship of Tufts University School of Medicine (TUSM) and Thieme Medical Publishers, New York. TUSM is accredited by the ACCME to provide continuing medical education for physicians.

**Credit:** Tufts University School of Medicine designates this journal-based CME activity for a maximum of **1 AMA PRA Category 1 Credit™**. Physicians should claim only the credit commensurate with the extent of their participation in the activity.

The American Cancer Society predicted there would be 226,160 new cases of lung cancer in 2012. Given that deaths from lung cancer account for nearly 28% of all cancer-related mortality, much attention has been paid to developing and improving treatment options to reverse outcomes of this grave disease.<sup>1</sup>

Percutaneous image-guided thermal ablation, collectively encompassing radiofrequency ablation (RFA), microwave ablation (MWA), and percutaneous cryotherapy, has emerged as a viable and potentially curative alternative to surgical resection for patients with primary and secondary malignancies of the lung. Thermal ablation has expanded the array of treatment options for patients with medical comorbidities precluding surgical resection and for inoperable patients with limited pulmonary reserve.

Different ablative technologies including radiofrequency, microwave, and cryoablation, and their relative roles, are addressed elsewhere in this issue of *Seminars*. However, since

**Issue Theme** Pulmonary Malignancies;  
Guest Editors, Bradley B. Pua, MD and  
David C. Madoff, MD, FSIR

Copyright © 2013 by Thieme Medical  
Publishers, Inc., 333 Seventh Avenue,  
New York, NY 10001, USA.  
Tel: +1(212) 584-4662.

DOI <http://dx.doi.org/10.1055/s-0033-1342957>.  
ISSN 0739-9529.

first reported by Dupuy et al in 2000, RFA has gained considerable traction in the treatment paradigm of non-resectable lung malignancies, both primary and secondary.<sup>2</sup> Microwave and cryoablation have emerged as promising alternatives and quite possibly represent the natural evolution of thermal ablation, whose impact remains to be seen.

Unlike surgery where histopathologic evaluation of the resected specimen can confirm a disease-free margin, because no specimen is obtained, uncertainty exists with thermal ablation about the adequacy of an ablative margin. Lethal ablation margins extending beyond the tumor are planned to include microscopic extent of disease that cannot be imaged but are pivotal to complete ablation.<sup>3</sup> Complete ablation is achieved using information acquired from computed tomography (CT) both prior to and during the ablation, combined with an understanding of the expected device-specific ablation zone and local factors, such as heat sinks, which can locally alter the extent of ablation and its effectiveness. Treatment adequacy is further confirmed with follow-up imaging, which uses characteristics such as size, enhancement, and fluorodeoxyglucose (FDG) uptake to determine treatment response and local control in addition to detection of disease beyond the locoregional landscape.

## Imaging Protocol following Thermal Ablation

Currently, no standard imaging protocol has been established or uniformly accepted. Several authors have recommended initial evaluation with contrast-enhanced CT within the first month of therapy and a variable pattern of alternating CT and positron emission tomography (PET)/CT every 3 months thereafter (►Fig. 1).<sup>4,5</sup> With the increasing utilization and acceptance of ablative techniques in treating unresectable primary and secondary pulmonary malignancies, a growing need has arisen to establish not only the optimal follow-up imaging protocol but also imaging references for assessing treatment response. The early identification of tumor recurrence, or tumor progression due to incomplete ablation, should enable the practitioner to offer expeditious retreatment or an alternative treatment.

The remainder of this review elaborates on the imaging findings following thermal ablation, both heat- and cold-based, of unresectable pulmonary malignancies. Given that the common pathologic end point of ablation, regardless of thermal energy used, is coagulation necrosis, many of the imaging findings are strikingly similar across the modalities.

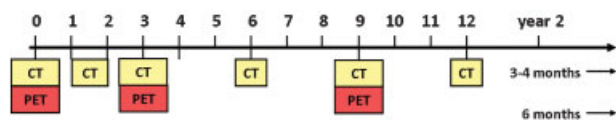


**Figure 1** Combined positron emission tomography/computed tomography (PET/CT) and CT modalities used in the follow-up imaging protocol after ablation. Initial PET/CT is required for staging. Thereafter, chest CT with CT nodule densitometry through the ablation zone is performed at 1 to 2 months, PET/CT at 3 months, and thereafter alternating every 3 months with chest CT for up to 2 years.

In general, the appearance of the ablation zone following radiofrequency and MWAs are quite similar, as might be expected given that both use heat energy, whereas the appearance of the ablation zone during and following cryoablation are similar but less well established within the medical literature. For simplicity, the imaging findings of the ablation zone caused by heat-based and cold-based techniques are discussed separately. Each energy-based section is subdivided into temporal phases following ablation: immediate/early (up to 1 week), intermediate (1 week to 2 months), and late (>2 months). Key differences are described.

## Radiofrequency and Microwave Ablation

### Immediate and Early Phase (<24 Hours to 1 Week)

#### Appearance of the Ablation Zone

During the later intraprocedural or immediate postprocedural period, a distinctive and reproducible pattern of concentric rings is expected. The central, or first, area of consolidation is surrounded by two layers, or rings; the inner, or second, is composed of concentric ground-glass opacity (GGO), and the outer, or third, of denser GGO. The central consolidation represents both the ablated tumor and the perilesional parenchyma that is necrotic, and on imaging it may be associated with intralesional bubbles<sup>6</sup> (►Fig. 2A–D). The presence of a margin of collective GGO is associated with treatment success, and lack thereof is associated with tumor progression due to incomplete ablation, as documented following both radiofrequency and MWA.<sup>2,7–10</sup> Yamamoto et al demonstrated that this peripheral GGO represents three distinct histopathologic layers, the outermost representing congested lung tissue and hemorrhage that retains its viability (►Fig. 2A–D). In fact, the peripheral GGO seen on CT overestimates the area of true coagulation necrosis by ~4.1 mm.<sup>11</sup> Given this overestimation, multiple authors have recommended an ablation margin, or peripheral GGO, of at least 5 mm to ensure adequate tumor kill following both radiofrequency and MWA.<sup>8,9,11</sup> Moreover, if a true 1-cm ablative margin is to be established, the GGO during and immediately following ablation should near 15 mm concentric to all margins of the targeted tumor. This “overablation” has been associated with higher rates of local control; de Baère et al concluded that an ablative area four times larger than the initial tumor is predictive of complete ablation.<sup>12</sup>

#### Size and Shape

The ablation zone size immediately following therapy should be larger than the index tumor for all thermal-based modalities because it includes both the tumor and the ablated perilesional lung tissue. This zone continues to enlarge during the first 24 hours<sup>13,14</sup> (►Fig. 2E). The development of hemorrhage or inflammation can lead to an apparent increased size of the ablation zone. As such, the Response Evaluation Criteria in Solid Tumors system of evaluating treatment response is generally not used following thermal ablation.<sup>15</sup>

The shape of the ablation zone is variable. Most often, it is ovoid or spherical. However, deviation from this is common and can be secondary to the number and placement of

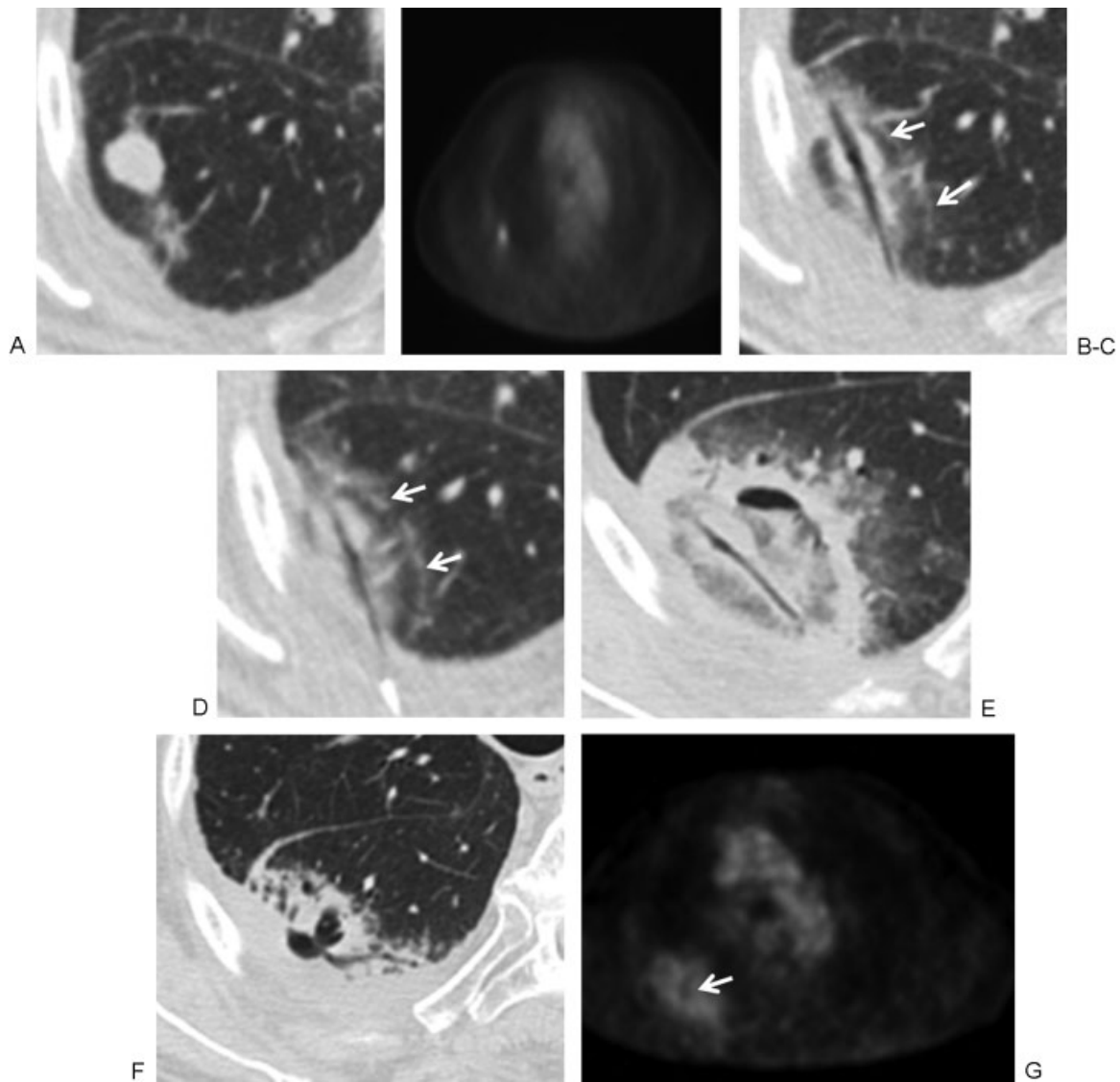


**Figure 2** (A, B) Computed tomography (CT) and positron emission tomography (PET) images of a 77-year-old man with adenocarcinoma of the lung in the superior segment of the right lower lobe obtained 1 week before ablation demonstrates a hypermetabolic nodule. (C, D) Microwave ablation (MWA) was performed with the patient in the prone position using a posterior approach and using 45 W for 7 minutes. Images are rotated to maintain continuity of lesion location. Immediately after the ablation there is central tissue desiccation and cavitation along the antennae tract. A second layer and rim of faint ground-glass opacity (GGO) surrounds the tumor and represents tissue necrosis. An outermost rim of denser GGO (white arrows) represents congested lung tissue and hemorrhage that retains viability. (E) Approximately 48 hours after MWA, there is an area of cavitation in the postablation zone, and the antennae tract remains desiccated. The ablation zone is larger than the pretreatment tumor and represents hemorrhage, edema, and necrotic tissue. With time the ablation zone should regress in size. (F, G) CT and PET at 6 weeks postablation. There is a decrease in size of the postablation zone and surrounding hemorrhage, with persistent central cavitation. The PET activity has returned to mediastinal blood pool activity with a central area of absent uptake corresponding to cavitation (arrow).

electrodes/antennas, the underlying shape of the index tumor, and, proximity to pleura, bronchi, or vessels. Proximity to the latter refers to the so-called heat sink phenomenon, which is associated with RFA more so than with MWA or cryoablation.<sup>16–19</sup>

#### Enhancement

Within the first week following thermal ablation, there is typically a marked reduction in contrast enhancement of the ablation zone, postulated to result from disruption of the microcirculation.<sup>20</sup> Wolf et al considered complete nonenhancement of the ablation zone on the initial scan to be

indicative of a successful MWA.<sup>9</sup> During this phase, a thin rim of enhancement, referred to as benign periablation enhancement, may be seen peripheral to the ablation zone; this rim is generally <5 mm thick and is concentric with smooth margins. This enhancement is believed to represent physiologic response to thermal injury—initially reactive hyperemia, and subsequently fibrosis and giant cell reaction.<sup>4,9,14</sup> Contrast-enhanced CT shows a peripheral thin rim of enhancement without central or nodular enhancement. Similarly, benign periablation enhancement has been observed following thermal ablation of both hepatic and renal malignancies.<sup>7,21–23</sup>

### Fluorodeoxyglucose-Positron Emission Tomography

Currently, <sup>18</sup>Fluorine (F)-FDG is the mainstay of PET oncologic imaging, including within the lung. Its limited specificity, however, precludes its use immediately following ablation given its propensity for inflammatory tissue, which is universally expected in this setting. In fact, early posttreatment PET within 4 days of RFA for stage IA non-small cell lung carcinoma was not found to be clinically useful in predicting overall event rates as compared with PET performed 6 months after ablation.<sup>24</sup>

### Complications

Complications of percutaneous thermal ablation are most often detected within the peri- and immediate postprocedural period. These can generally be divided into pleural-based and parenchymal-based complications.

Pleural-based complications include pneumothorax (most common), pleural effusion, hemothorax, and pleural thickening.<sup>25</sup> In a meta-analysis by Chan et al of 46 published studies with a total of 2905 patients, the most common side effect or complication was pneumothorax (28.3%), followed by pleural effusions (14.8%).<sup>26</sup> In general, the reported rate of pneumothorax occurrence following radiofrequency and MWA ranges between 30% and 50%.<sup>4,9,27-29</sup> Given both the inherent risk of introducing a large-bore needle across the pleura and the high prevalence of underlying emphysema in patients with lung cancer, some incidence of pneumothorax should always be anticipated.

The rate of pneumothorax in patients undergoing ablation that requires chest tube placement has been reported to range from 0% to 54%, although the latter percentage included patients who underwent thoracotomy and subsequent automatic chest tube placement. Many studies have reported chest tube placement in <25% of pneumothoraces.<sup>6,20,28,29</sup> Ablation of peripheral tumors can be particularly challenging and sometimes problematic due to the inherent infliction of

pleural injury and the extreme desiccation that occurs with ablation, in particular with microwave energy that is thought to be associated with an increased rate of bronchopleural communication (►Fig. 3).<sup>30,31</sup>

Radiographically apparent parenchymal-based complications include pulmonary hemorrhage, although some degree of minor hemorrhage should be expected during ablation because tissues are destroyed. Other complications that have been reported include pneumonia and abscess formation,<sup>25</sup> but in practice these are relatively uncommon, reported at 1.5% and 0.4%, respectively.<sup>26</sup> On rare occasions, ablation has cascaded into acute respiratory distress syndrome, its onset appearing outside the immediate periprocedural time frame.

### Intermediate Phase (1 Week to 2 Months)

#### Appearance of the Ablation Zone

The GGO seen immediately following thermal ablation is expected to involute by 1 to 3 months<sup>21,32</sup> (►Fig. 2F).

Cavitation within the ablation zone, which has been considered a positive response to thermal ablation, is most likely to appear in the intermediate postablation phase.<sup>9,14</sup> Pretreatment factors that favor cavitation include central location, juxtaposition to a segmental bronchus, and ablation size >2.8 cm.<sup>32</sup> Cavitation has been postulated to be secondary to the drainage of necrotized tissue by adjacent bronchi, with preservation of the outermost "rigid" layer of the ablation zone.<sup>11</sup> Bojarski et al reported a 31% prevalence of bubble lucencies, defined as 1- to 3-mm gas bubbles within the ablation zone during the follow-up period. Of note, in this series all but one patient demonstrated complete resolution of the gas bubbles at 1-year follow-up.<sup>32</sup>

Although adjacent pleural thickening can be seen within the immediate postablation phase, it is more likely to manifest within the intermediate phase and most often involves the portion of pleura traversed by the ablation probe.<sup>32</sup>

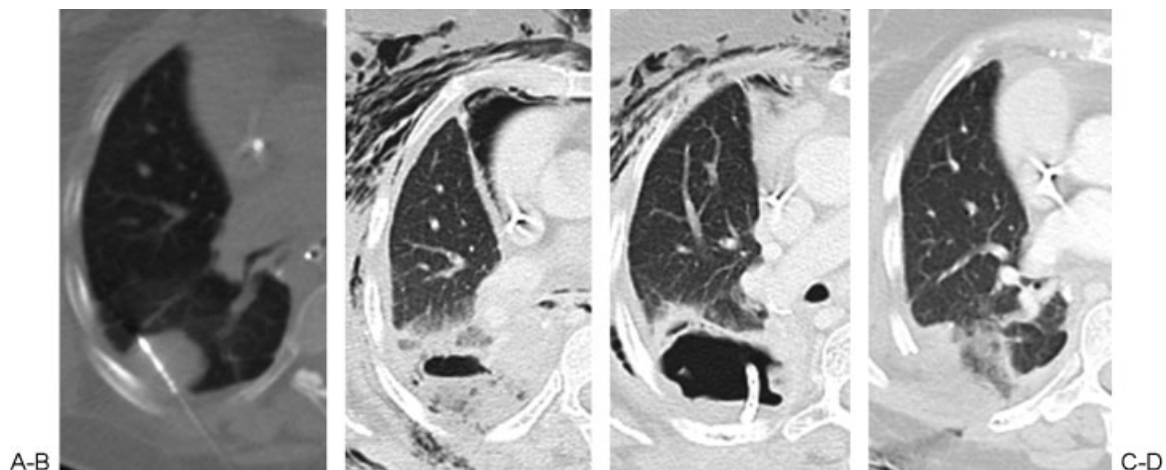


**Figure 3** (A) A 50-year-old woman with metastatic uterine leiomyosarcoma. Microwave ablation of a pleural-based right lung metastasis at the inferior edge of a prior radiation treatment. (B, C) By the second postprocedure day, the patient developed fever and extensive subcutaneous emphysema, with computed tomography showing necrotizing postablation zone and air track to subcutaneous tissue from a bronchopleural fistula. A drainage tube was placed in the cavity. The patient was taken to the operating room for debridement and rib resection. Four weeks after the procedure and surgical debridement, there was near complete resolution of the bronchopleural fistula and subcutaneous emphysema (not shown). (Courtesy of Dr. Majid Maybody.)

Hilar or mediastinal lymph node hyperplasia can occur during this period with resultant lymph node enlargement and FDG uptake. Reported in up to 63% of RFA cases, this nodal enlargement is transient, often resolving by 1 year. Interestingly, the appearance of enlarged lymph nodes is unpredictable and lacks correlation with initial tumor size and location.<sup>22</sup> Lymph node enlargement has likewise been reported following MWA but again is not associated with local recurrence or all-cause mortality,<sup>9</sup> lending credence to the notion that enlarged lymph nodes more likely represent reactive change and not necessarily disease recurrence or progression. Consequently, the presence of enlarged reactive lymph nodes can potentially confound the evaluation for locoregional recurrence, so it is important to bear this possibility in mind when evaluating posttreatment scans.

### Size and Shape

For the most part, the ablation zone should remain larger than the pretreatment tumor during the intermediate phase after ablation, but it often demonstrates reduced size compared with the immediate postprocedure scan (►Fig. 2F). This likely reflects regression of parenchymal edema, inflammation, and hemorrhage.<sup>4</sup>

Although the World Health Organization reporting criteria deemed an enlargement of 25% compared with prior imaging as a significant predictor for residual or recurrent disease, this and other methods of disease quantification are rendered suboptimal given several confounding factors. These factors include periablation inflammation or hemorrhage and the development of cavitation, all of which artificially inflate single or bidimensional measures. In practice, size alone cannot be considered the definitive assessment of incomplete ablation or tumor progression. In the subsequent phase of follow-up, however, allowing for inflammatory effects to subside, a continued increase in ablation zone size should raise suspicion for inadequate control and tumor recurrence. Isolated stabilization or expansion of ablation zone size during this phase should not be considered an indicator of tumor recurrence.<sup>25</sup>

### Enhancement

As within the immediate phase following ablation, ablation zone enhancement within the intermediate phase should remain markedly less than that seen within the tumor prior to treatment. Although benign periablation enhancement can persist for up to 6 months, the appearance of central or nodular enhancement >10 mm and/or 15 HU during this phase may herald progression of incompletely ablated disease.<sup>4,9,14,20</sup>

### FDG-PET

Peak uptake of <sup>18</sup>F-FDG typically occurs by 2 weeks following ablation. By 2 months, ablation zone uptake should return to that of the mediastinal blood pool (►Fig. 2G). Okuma et al showed that at 2 months, persistent FDG uptake or uptake that is not reduced by at least 60% from baseline may predict radiographic recurrence at 6 months.<sup>23</sup> Singnurkar et al defined six uptake patterns at PET/CT performed between 1 and 4 months after ablation: (1) diffuse, (2) focal, (3) hetero-

geneous, (4) rim, (5) rim plus focal uptake corresponding to the site of the original lesion, and (6) rim plus focal uptake at a different location (not corresponding to the site of the original lesion). Favorable uptake patterns included rim, diffuse, heterogeneous, and rim plus focal uptake when the focal uptake did not correspond to the original tumor nodule. Rim with superimposed focal uptake corresponding to the original tumor nodule was shown to be associated with local recurrence. Superimposed focal uptake at a noncorresponding site was hypothesized to indicate heterogeneous inflammation around the ablated site.<sup>33</sup>

### Complications

Pneumothoraces that were present during the immediate phase often become localized, and on occasion they evolve into contained bronchopleural fistulae. Their appearance is more disconcerting than clinically relevant<sup>30,32,34</sup> (►Fig. 3). Problematic bronchopleural fistulae are more likely to manifest within this intermediate postablation phase.<sup>30,32,34</sup> Pleural effusions that were initially present would typically begin to involute at this point, but initial appearance during this period is also not uncommon.

### Late Phase (>2 Months)

#### Appearance of the Ablation Zone

The ablation zone continues to involute during this period and ultimately may even disappear with only parenchymal scarring remaining in its place.

Radiographic findings characteristically seen during the immediate and intermediate phases typically resolve or significantly improve during this late period. These include parenchymal features, specifically cavitation, and pleural changes, such as pleural thickening, pleural effusion and localized pneumothorax, or contained bronchopleural fistula.

During this phase, perhaps even more than during the early and intermediate phases, the development of satellite nodules or new nodules along the prior electrode/antenna track portends new local or locoregional disease.

#### Size and Shape

In general, the size of the ablation zone at 3 months is the same or larger than the baseline tumor followed by continued volume reduction to 6 months. After 6 months, it is reasonable to expect the size of the ablation zone to be smaller than the baseline tumor secondary to involution of local hemorrhagic and inflammatory effects.<sup>2,14,32,35</sup> Within this phase, the postablation zone may regress to scar, nodular scar, or even a thin-walled cavity. Continually increasing or newly enlarging ablation zone beyond 3 months and definitively beyond 6 months is highly suggestive for tumor recurrence and progressive local disease<sup>14</sup> (►Fig. 4). Delayed recurrence or tumor progression due to more effective tumor kill even beyond 1 year warrant and reinforce the importance of continued clinical and imaging follow-up.

#### Enhancement

Mean contrast enhancement of the ablation zone at 3 months can be greater than that seen within the immediate or

intermediate phases. This is postulated to be secondary to recovery of the microcirculation, not recurrence of the tumor.<sup>20</sup> Regardless, overall contrast enhancement should never exceed that of the index tumor, and after 6 months enhancement should continue to decrease and not exceed the enhancement at 3 months. As during the intermediate phase, the appearance and/or continuation of central or nodular enhancement >10 mm and/or 15 HU suggests progression of incompletely ablated disease.<sup>20</sup>

#### FDG-PET

Increased metabolic activity after 2 months, new uptake at the site of the previously ablated tumor, or activity within the center of the ablation zone are all findings concerning for tumor recurrence<sup>4</sup> (►Fig. 4 F).

## Cryoablation

### Immediate and Early Phase (<24 Hours to 1 Week)

#### Appearance of the Ablation Zone

One benefit of cryoablation is the ability to visualize the ice ball throughout the periprocedural period. Many groups have described difficulty visualizing ice ball formation within the lung due to the inability to see low-density ice against a

background of air<sup>14,36</sup> further obscured by perilesional hemorrhage.<sup>37</sup> In our experience, the extent of ice formation is readily visualized following the initial thaw cycle when hemorrhage develops along the margins of the ablation zone. CT imaging during subsequent freeze cycles clearly delineates a low-density ovoid ice ball within the background of higher attenuated hemorrhage (►Fig. 5A–C).

Multiple studies have shown that the ice ball seen during the procedure overestimates the extent of coagulation necrosis by as much as 4 to 5 mm, as confirmed on histopathologic specimens. This occurs because the edge of the ice ball corresponds to the 0°C isotherm, which is not cytotoxic.<sup>38,39</sup> The –20°C isotherm is typically several millimeters within the edge of the ice ball and more reliably demarcates the extent of complete coagulation necrosis.<sup>38,39</sup> As ice melts at the completion of the ablation, a zone of ground glass and consolidation forms around the ablation zone, which is secondary to a combination of coagulation necrosis and hemorrhage. During this time, the size of the ablation zone is always larger than the targeted tumor (►Fig. 5D, E).

Over the course of the first week, much of the peripheral ground glass and consolidation resolves, reflecting resolution of most of the periablation edema and hemorrhage. The ablation zone becomes more contained and is delineated from the adjacent nonablated lung by a thin rim<sup>14</sup>

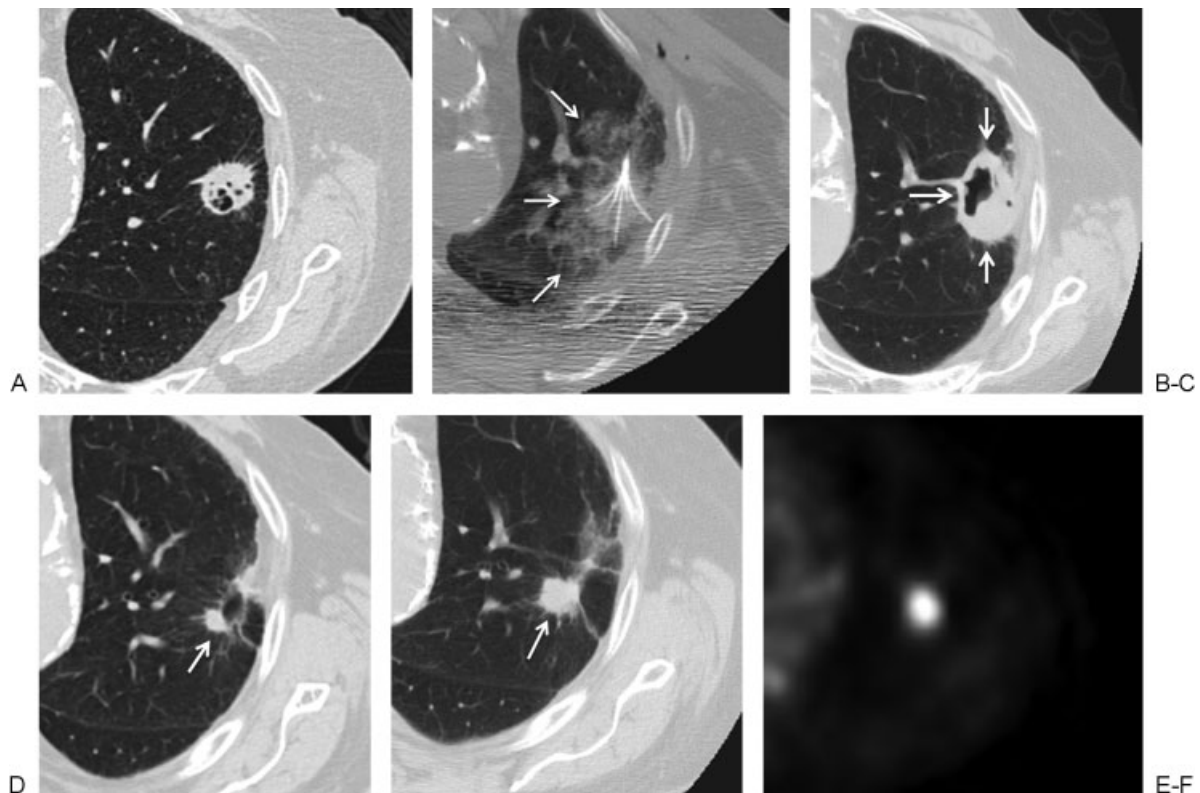


**Figure 4** (A, B) An 84-year-old man with a biopsy-proven cavitary left upper lobe squamous cell carcinoma. Based on significant cardiovascular risk factors precluding surgical resection, the patient was referred for radiofrequency ablation. A multi-array electrode was used to perform overlapping ablations at 3 cm and 4 cm, each for 15 minutes. (B) The intra-ablation imaging demonstrated a rim of ground glass (white arrows) completely surrounding the mass. (C) At 5 weeks following treatment, the ablation zone (white arrows) consists of eccentric cavitation, covering the extent of the target lesion. (D) By 6 months, a nodule (white arrow) remains along the margin of the otherwise fully scarred ablation zone. (E, F) At 13 months, this nodule has grown (white arrow) and displays intense fluorodeoxyglucose uptake on positron emission tomography, compatible with residual tumor.

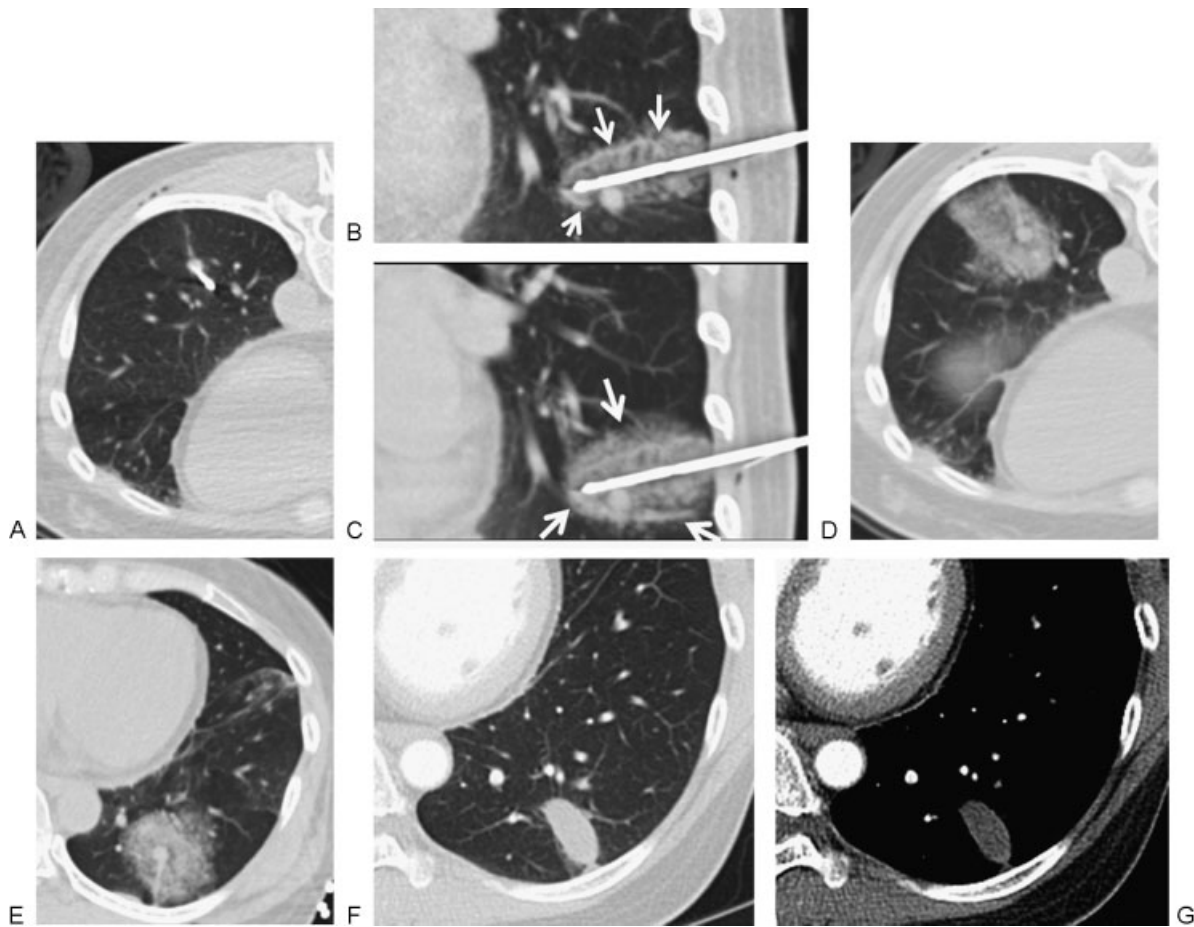


**Figure 5** (A) A 50-year-old woman with solitary metastatic colon carcinoma to left lower lobe. Multiple attempts were made to place the probe through the nodule; however, the nodule changed position, a common finding while placing larger cryoprobes in smaller subcentimeter nodules. Ultimately the cryoprobe was placed at the superior surface of the nodule. (B) Initial 3 minutes of freeze cycle followed by passive thaw was performed to create hemorrhage surrounding the nodule and to allow for the definite freeze cycle. Peripheral rim of hyperdensity represents the edge of the melting ice ball (arrows), and the inner hypodensity surrounding the probe represents the ice ball itself. (C) Following a second freeze cycle of 10 minutes, the edge of the ice ball is seen (arrow) extending beyond the initial hemorrhage. (D) Immediately postablation, there is development of hemorrhage at the ablation site representing necrosis and hemorrhage. (E) The patient was placed in a supine position to limit the transbronchial spread of hemorrhage. (F, G) At 1 week following cryoablation, computed tomography demonstrates an elliptical ablation zone with resolution of hemorrhage. The size of the ablation zone is larger than the ablated nodule and depends on the number and size of the original ablation probes.

(► **Fig. 5F, G**). Cavitation may occur during this time, just as with the heat-based ablations.

#### Size and Shape

The size of the cryoablation zone is determined by the cryoprobe type, number and positioning, and the number of freeze-thaw cycles. Each commercially available cryoprobe comes with a prospectus that describes the extent of ice ball formation, as well as the size of cytotoxic isotherms, typically based on in vitro models. The length and width of the ablation zone are proportional to the length and width of the cooled portion of the cryoprobe, and as such a longer active length of the cryoprobe will result in an elliptical ablation, whereas a shorter length will result in a more spherical ablation (► **Fig. 5F, G**). Overlapping ablations performed with multiple cryoprobes are at least additive in increasing the size of the ablation, and in some cases they can lead to a very large

ablation zone by limiting the effects of local thermal sinks (► **Fig. 6**).

The shape of the ablation is most significantly affected by thermal sinks, with blood vessels measuring  $>3$  mm serving as the most effective thermal sinks; large and medium-size airways can impart a similar effect. As with heat-based ablations, the margins of a cryoablation zone will be contoured by the presence of a neighboring thermal sink. When the targeted tumor abuts a thermal sink, a sufficient ablation may be difficult to achieve, rendering recurrence more likely to occur (► **Fig. 7**).

By altering thermal conductivity, local hemorrhage not only provides a medium by which to advantageously visualize the ice ball during ablation but enhances expansion of the cryoablation zone and ultimately creates a larger ablation zone. This synergy is further exploited with triple-freeze protocols<sup>40</sup> (► **Fig. 5B, C**).

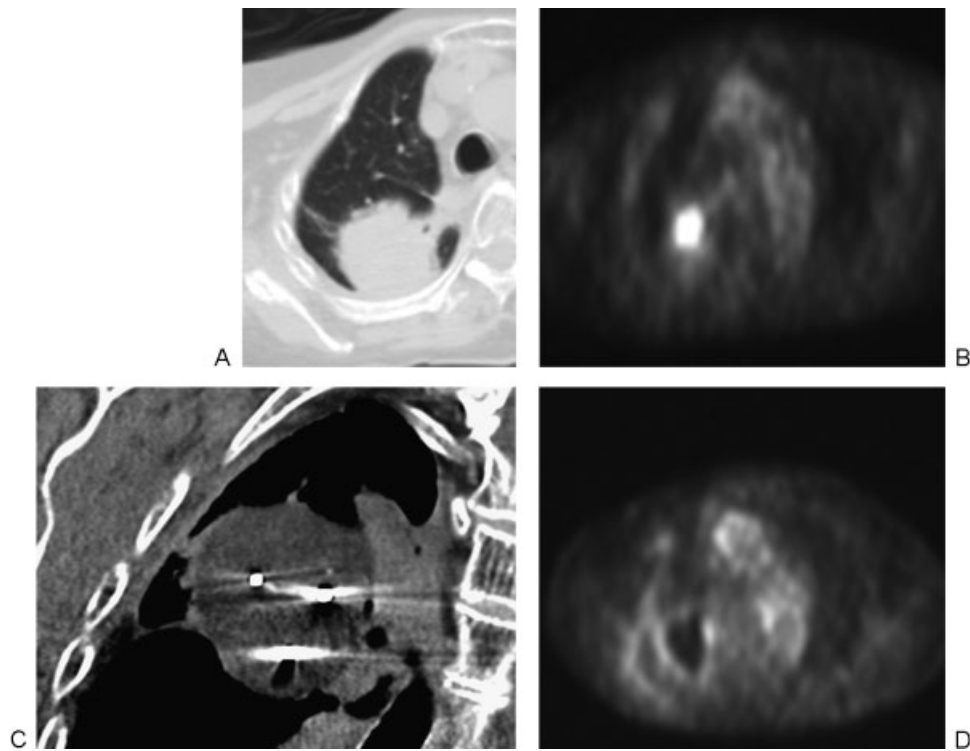


**Figure 6** (A, B) A 90-year-old woman with history of primary lung carcinoma status postradiation, with recurrence of the tumor. High central metabolic activity is noted on positron emission tomography (PET). (C) Three probes were placed in the mass. Simultaneous cryoablation was performed with the ice balls (arrow), merging to create a large ablation zone. (D) At 2 months postablation, PET scan demonstrated a central metabolic area with thin rim of metabolic activity not exceeding that of the mediastinum. Despite a presumed favorable response, PET should be repeated in 6 months to confirm absence of residual tumor.

### Enhancement

Enhancement along the ablation zone margin can be seen in up to a third of ablation zones immediately following ablation and subsequently fades with time.<sup>14</sup> In a small percentage of individuals, internal enhancement within the ablation zone can be seen, but this enhancement disappears by 1 month.<sup>14</sup>

### FDG-PET

As with radiofrequency and MWAs, PET has no role in early postprocedure evaluation following cryoablation. In our experience, the potential metabolic activity associated with

residual or incompletely ablated tumor is impossible to distinguish from the diffuse activity of inflammation throughout the ablation zone.

### Complications

The potential complications associated with cryoablation do not substantially differ from those of heat-based ablation and include pneumothorax, pleural effusion and hemorrhage, and pulmonary hemorrhage. As compared with heat-based ablation, pulmonary hemorrhage and hemoptysis occur at a higher frequency than with cryoablation (→Fig. 5D, E) due

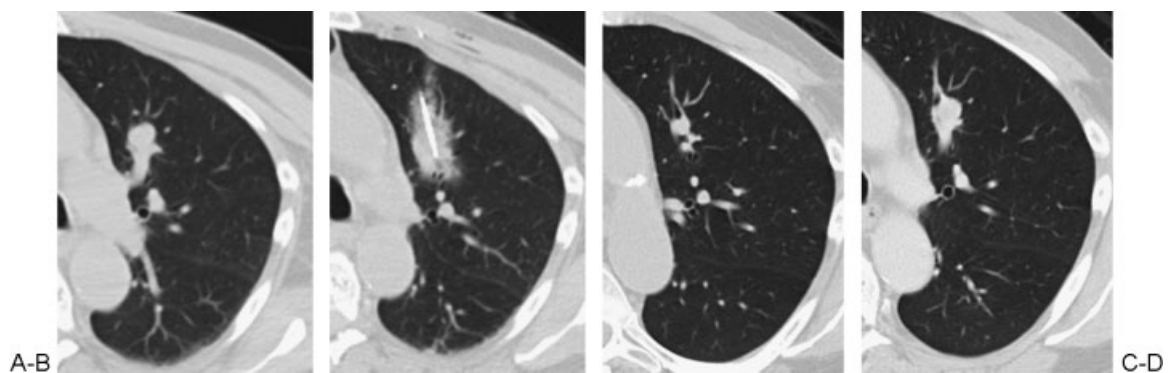


**Figure 7** (A) Metastatic renal cell carcinoma to the left upper lobe, with a larger vessel (4 mm) in close proximity of the metastasis. (B) Following two cycles of ablation, the ice ball and cryo-zone did not grow to an expected size, despite prolonged ablation. It is hypothesized that the vessel adjacent to the nodule and ablation zone may have contributed to a cold sink effect. (C) At 1-month follow-up computed tomography scan, the size of the nodule is smaller but remains nodular. (D) At 5 months the nodule had grown, suggestive of recurrence.



to two principal factors. First, breakdown and fracture of now fragile small blood vessels occur as the ice ball melts, releasing blood and melting ice into adjacent alveolar sacs and bronchi. Second, cryotherapy lacks the cautery effect inherent in heat-based ablation, and in situations of borderline coagulation status and coagulopathy, radiofrequency and microwave energies are generally preferred.

Pleural effusion or hemorrhage can occur during the early or late phases following cryoablation, typically when the ablation is performed in a peripheral location adjacent to the pleura. When the pleural effusion presents during the immediate periprocedural period, it often has a hemorrhagic component and will have increased attenuation on CT. Pleural effusions that present days after the procedure are more likely to be reactive, and although they may contain blood are unlikely to be frankly hemorrhagic. In some cases, however, these pleural effusions may be symptomatic and require drainage (►Fig. 8).

### Intermediate Phase (1 Week to 2 Months)

#### Appearance of the Ablation Zone

The GGO surrounding the ablation zone resolves by the end of the first month.<sup>14</sup> Cavitation is common and likely to persist during most of, if not the entire, intermediate phase.<sup>35</sup> In general, the appearance of the cryoablation zone during the intermediate phase does not substantially differ from that observed following heat-based ablation, and as expected with heat-based energies, the cryoablation zone during this phase should not demonstrate enlargement (►Fig. 9).

#### Size and Shape

During the intermediate period, the cryoablation zone becomes more discrete and rounded with increasingly well-delineated margins. Involution of the ablation zone begins during the first 2 months following cryotherapy. In one study, Ito et al showed that all 79 ablation zones decreased in size at



**Figure 8** (A) Axial prone computed tomography (CT) image demonstrates a peripheral right lower lobe metastasis in this patient with colon cancer. (B, C) Axial prone and coronal CT images demonstrate two cryoprobes placed in the mass with multiple layering ice balls, indicating the multiple cycles of ablation. (D) 1 week following initial ablation, the patient presented for repeat ablation but was found to have a large pleural effusion. The effusion was drained, and repeat ablation was performed.

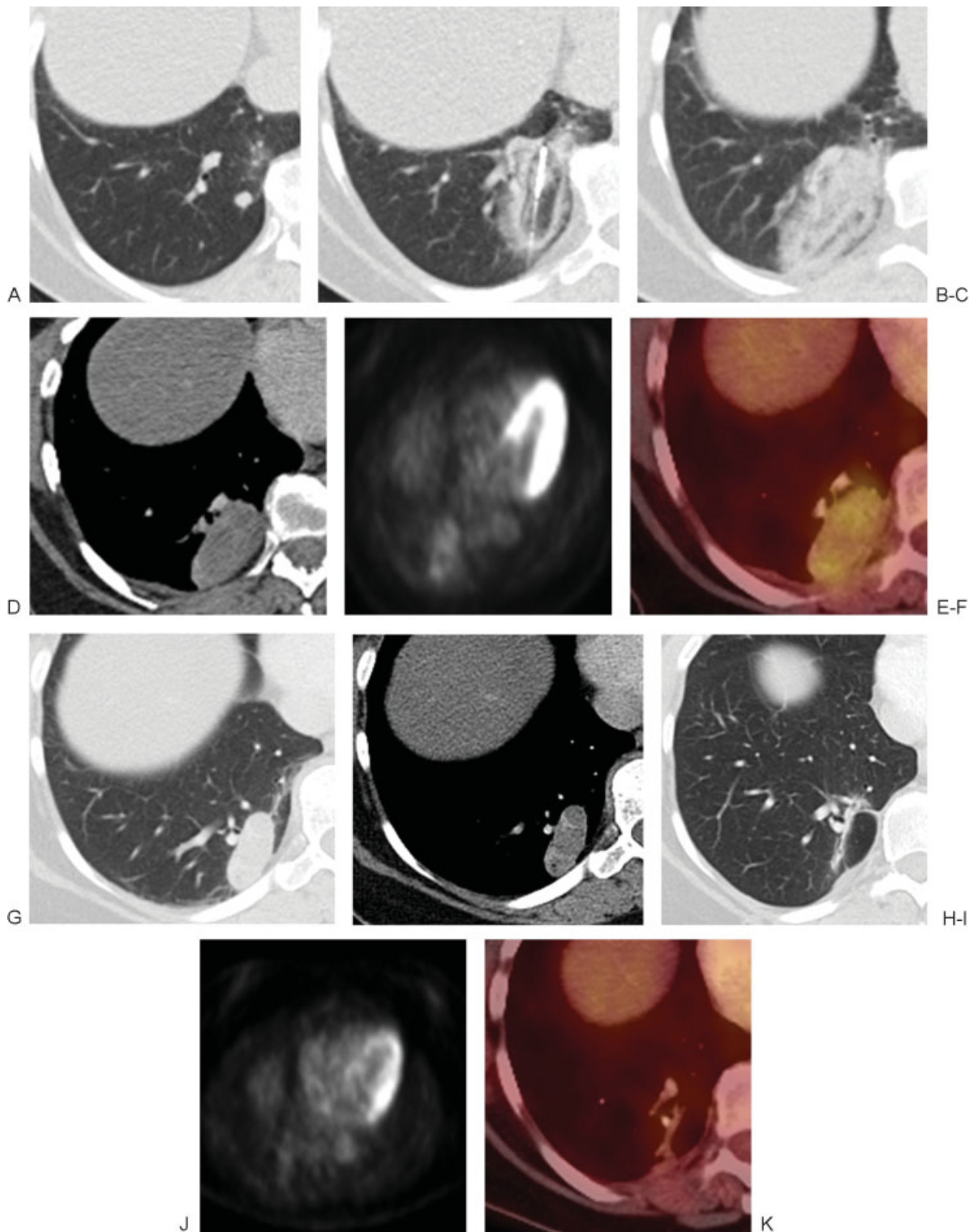


**Figure 9** (A) Metastatic renal cell carcinoma to the right lower lobe. (B) A single cryoprobe was used to ablate the lesion. Alternating circumferential layers of different intensities within the ice ball are seen engulfing the tumor. (C) Immediately postablation, the patient was placed in a supine position to limit hemorrhage into surrounding structures. A postablation zone with associated hemorrhage engulfs the initial tumor. (D–F) Follow-up at 1 month with (D) computed tomography (CT), (E) positron emission tomography (PET), and (F) fused CT/PET scans demonstrate an oval postablation zone with thin rim of peripheral enhancement and mild internal metabolic activity. (G, H) CT scan obtained 6 months after the ablation demonstrates oblong postablation zone with thin rim of peripheral enhancement. (I–K) Follow-up at 11 months with (I) CT, (J) PET, and (K) fused CT/PET scans demonstrate significant decrease in size of the ablation zone to a slit-like scar with no metabolic activity.

1 and 3 months following cryoablation.<sup>14</sup> Any increase in size occurring during the first 2 months should be viewed with suspicion for residual disease, particularly if this enlargement is accompanied with nodular growth within the ablation zone or at its margins (►Fig. 9D–F).

### Enhancement

During the intermediate phase, marginal enhancement of the cryoablation zone can be seen and gradually fades with only minimal enhancement expected by the end of 2 months (►Fig. 9D). As with heat-based ablation zones, contrast enhancement should never exceed that of the original tumor, and for the most part any increase in enhancement, especially if central or nodular, is concerning for tumor progression.

### FDG-PET

The appearance of the cryoablation zone with PET imaging has not been well described nor its timing established within the medical literature. In our experience, metabolic imaging of the ablation zone within the first 2 months following cryoablation demonstrates a sharper drop in signal when compared with heat-based ablative techniques. A peripheral rim of activity or amorphous FDG uptake within the ablation zone can be present, presumably due to inflammation, and it is more often confusing than useful as a marker for complete ablation or as an early predictor for incomplete ablation (►Fig. 6D and 9).

### Late Phase (>2 Months)

#### Appearance of the Ablation Zone

During the late phase, the cryoablation zone continues to maintain its well-marginated consolidative appearance, and over time the cryoablation zone involutes until only a linear band of parenchymal scar remains (►Fig. 9I–K). By 3 months, most of the cavitation has resolved, suggesting resorption of necrotic debris.<sup>35</sup> In some instances, however, cavitation may persist up to 9 months.<sup>35</sup>

#### Size and Shape

Ablation zones progressively decrease after 1 month<sup>35</sup> (►Fig. 9). Continued enlargement of the cryoablation zone after 6 months is highly suggestive for tumor recurrence.<sup>14</sup> In our experience, for any given ablation size and relative ablation size to tumor size, involution of the cryoablation zone occurs earlier and more rapidly, when compared with those following radiofrequency and MWAs. This allows for potentially earlier detection of tumor progression, a conceivable competitive advantage with cryotherapy over heat-based therapies. Based on current data, it is unclear where timelines for ablation zone size reduction should be set. As with radiofrequency ablation, the trajectory of the ablation zone size must be followed, and increasing size or nodularity after previously documented involution is concerning for tumor progression.

### Enhancement

During the late phase, internal and particularly marginal enhancement can be seen for up to 6 months (►Fig. 9).

Although the degree of enhancement was not detailed, Ito et al showed that all patients with internal enhancement of their ablation zones beyond 6 months had incompletely ablated and progressive disease.<sup>14</sup>

### FDG-PET

Compared with CT alone, PET/CT is preferably used for detection of late recurrence of disease because it allows assessment of not only the locoregional site, including the cryoablation zone, but the entire body for new distant sites of disease. Although the appearance of the cryoablation zone has not been well described, its metabolic appearance is likely akin to that of the RFA zone (►Fig. 9I–K). Tracer activity above the threshold of the original tumor, increasing on serial imaging or developing within the central core of the ablation zone, is suspicious for recurrent disease.

## Conclusion

Reliable imaging surveillance after thermal ablation is essential and remains a mainstay for its continued success. A firm understanding of the expected and unexpected imaging features of the ablation zone, regardless of thermal energy source used, is critical for accurate assessment of treatment response and early identification of incomplete ablation, and locoregional and/or distant progression of disease. Nonenhanced and contrast-enhanced CT, PET, and PET/CT should be used in conjunction as routine follow-up or as problem-solving modalities, and although not specifically addressed within the confines of this article, biopsy should be entertained whenever imaging findings are equivocal. Even with 100% local control, an already predetermined number of treated individuals will have microscopic disease beyond their ablated tumor that is below the detection of currently available imaging techniques. This, further exacerbated by high-risk patient populations in which pathologic staging is unavailable, should drive diligent and rigorous patient follow-up.

## References

- 1 Surveillance Epidemiology and End Results (SEER). Available at : [http://seer.cancer.gov/csr/1975\\_2009\\_pops09/](http://seer.cancer.gov/csr/1975_2009_pops09/)
- 2 Dupuy DE, Zagoria RJ, Akerley W, Mayo-Smith WW, Kavanagh PV, Safran H. Percutaneous radiofrequency ablation of malignancies in the lung. *AJR Am J Roentgenol* 2000;174(1):57–59
- 3 Giraud P, Antoine M, Larrouy A, et al. Evaluation of microscopic tumor extension in non-small-cell lung cancer for three-dimensional conformal radiotherapy planning. *Int J Radiat Oncol Biol Phys* 2000;48(4):1015–1024
- 4 Abtin FG, Eradat J, Gutierrez AJ, Lee C, Fishbein MC, Suh RD. Radiofrequency ablation of lung tumors: imaging features of the postablation zone. *Radiographics* 2012;32(4):947–969
- 5 Beland MD, Wasser EJ, Mayo-Smith WW, Dupuy DE. Primary non-small cell lung cancer: review of frequency, location, and time of recurrence after radiofrequency ablation. *Radiology* 2010;254(1):301–307
- 6 Hiraki T, Tajiri N, Mimura H, et al. Pneumothorax, pleural effusion, and chest tube placement after radiofrequency ablation of lung tumors: incidence and risk factors. *Radiology* 2006;241(1):275–283

- 7 Gazelle GS, Goldberg SN, Solbiati L, Livraghi T. Tumor ablation with radio-frequency energy. *Radiology* 2000;217(3):633–646
- 8 Anderson EM, Lees WR, Gillams AR. Early indicators of treatment success after percutaneous radiofrequency of pulmonary tumors. *Cardiovasc Intervent Radiol* 2009;32(3):478–483
- 9 Wolf FJ, Grand DJ, Machan JT, Dipetrillo TA, Mayo-Smith WW, Dupuy DE. Microwave ablation of lung malignancies: effectiveness, CT findings, and safety in 50 patients. *Radiology* 2008;247(3):871–879
- 10 Lee JM, Jin GY, Goldberg SN, et al. Percutaneous radiofrequency ablation for inoperable non-small cell lung cancer and metastases: preliminary report. *Radiology* 2004;230(1):125–134
- 11 Yamamoto A, Nakamura K, Matsuoka T, et al. Radiofrequency ablation in a porcine lung model: correlation between CT and histopathologic findings. *AJR Am J Roentgenol* 2005;185(5):1299–1306
- 12 de Baère T, Palussière J, Aupérin A, et al. Midterm local efficacy and survival after radiofrequency ablation of lung tumors with minimum follow-up of 1 year: prospective evaluation. *Radiology* 2006;240(2):587–596
- 13 Vogl TJ, Naguib NN, Gruber-Rouh T, Koitka K, Lehnert T, Nour-Eldin NE. Microwave ablation therapy: clinical utility in treatment of pulmonary metastases. *Radiology* 2011;261(2):643–651
- 14 Ito N, Nakatsuka S, Inoue M, et al. Computed tomographic appearance of lung tumors treated with percutaneous cryoablation. *J Vasc Interv Radiol* 2012;23(8):1043–1052
- 15 Therasse P, Arbuck SG, Eisenhauer EA, et al. New guidelines to evaluate the response to treatment in solid tumors. European Organization for Research and Treatment of Cancer, National Cancer Institute of the United States, National Cancer Institute of Canada. *J Natl Cancer Inst* 2000;92(3):205–216
- 16 Goldberg SN, Grassi CJ, Cardella JF, et al; Society of Interventional Radiology Technology Assessment Committee; International Working Group on Image-Guided Tumor Ablation. Image-guided tumor ablation: standardization of terminology and reporting criteria. *Radiology* 2005;235(3):728–739
- 17 Hinshaw JL, Lee FT Jr. Cryoablation for liver cancer. *Tech Vasc Interv Radiol* 2007;10(1):47–57
- 18 Simon CJ, Dupuy DE, Mayo-Smith WW. Microwave ablation: principles and applications. *Radiographics* 2005;25(Suppl 1):S69–S83
- 19 Wright AS, Sampson LA, Warner TF, Mahvi DM, Lee FT Jr. Radiofrequency versus microwave ablation in a hepatic porcine model. *Radiology* 2005;236(1):132–139
- 20 Suh RD, Wallace AB, Sheehan RE, Heinze SB, Goldin JG. Unresectable pulmonary malignancies: CT-guided percutaneous radiofrequency ablation—preliminary results. *Radiology* 2003;229(3):821–829
- 21 Steinke K, King J, Glenn D, Morris DL. Radiologic appearance and complications of percutaneous computed tomography-guided radiofrequency-ablated pulmonary metastases from colorectal carcinoma. *J Comput Assist Tomogr* 2003;27(5):750–757
- 22 Sharma A, Digumarthy SR, Kalra MK, Lanuti M, Shepard JA. Reversible locoregional lymph node enlargement after radiofrequency ablation of lung tumors. *AJR Am J Roentgenol* 2010;194(5):1250–1256
- 23 Okuma T, Okamura T, Matsuoka T, et al. Fluorine-18-fluorodeoxyglucose positron emission tomography for assessment of patients with unresectable recurrent or metastatic lung cancers after CT-guided radiofrequency ablation: preliminary results. *Ann Nucl Med* 2006;20(2):115–121
- 24 Yoo DC, Dupuy DE, Hillman SL, et al. Radiofrequency ablation of medically inoperable stage IA non-small cell lung cancer: are early posttreatment PET findings predictive of treatment outcome? *AJR Am J Roentgenol* 2011;197(2):334–340
- 25 Rose SC, Thistlethwaite PA, Sewell PE, Vance RB. Lung cancer and radiofrequency ablation. *J Vasc Interv Radiol* 2006;17(6):927–951; quiz 951
- 26 Chan VO, McDermott S, Malone DE, Dodd JD. Percutaneous radiofrequency ablation of lung tumors: evaluation of the literature using evidence-based techniques. *J Thorac Imaging* 2011;26(1):18–26
- 27 Kawamura M, Izumi Y, Tsukada N, et al. Percutaneous cryoablation of small pulmonary malignant tumors under computed tomographic guidance with local anesthesia for nonsurgical candidates. *J Thorac Cardiovasc Surg* 2006;131(5):1007–1013
- 28 Gillams A. Tumour ablation: current role in the kidney, lung and bone. *Cancer Imaging* 2009;(9 Spec No A):S68–S70
- 29 Yamakado K, Hase S, Matsuoka T, et al. Radiofrequency ablation for the treatment of unresectable lung metastases in patients with colorectal cancer: a multicenter study in Japan. *J Vasc Interv Radiol* 2007;18(3):393–398
- 30 Cannella M, Cornelis F, Descat E, et al. Bronchopleural fistula after radiofrequency ablation of lung tumours. *Cardiovasc Intervent Radiol* 2011;34(Suppl 2):S171–S174
- 31 Bui JT, Gaba RC, Knuttinen MG, et al. Microwave lung ablation complicated by bronchocutaneous fistula: case report and literature review. *Semin Intervent Radiol* 2011;28(2):152–155
- 32 Bojarski JD, Dupuy DE, Mayo-Smith WW. CT imaging findings of pulmonary neoplasms after treatment with radiofrequency ablation: results in 32 tumors. *AJR Am J Roentgenol* 2005;185(2):466–471
- 33 Singnurkar A, Solomon SB, Gönen M, Larson SM, Schöder H. 18F-FDG PET/CT for the prediction and detection of local recurrence after radiofrequency ablation of malignant lung lesions. *J Nucl Med* 2010;51(12):1833–1840
- 34 Sakurai J, Hiraki T, Mukai T, et al. Intractable pneumothorax due to bronchopleural fistula after radiofrequency ablation of lung tumors. *J Vasc Interv Radiol* 2007;18(1 Pt 1):141–145
- 35 Wang H, Littrup PJ, Duan Y, Zhang Y, Feng H, Nie Z. Thoracic masses treated with percutaneous cryotherapy: initial experience with more than 200 procedures. *Radiology* 2005;235(1):289–298
- 36 Saliken JC, McKinnon JG, Gray R. CT for monitoring cryotherapy. *AJR Am J Roentgenol* 1996;166(4):853–855
- 37 Izumi Y, Oyama T, Ikeda E, Kawamura M, Kobayashi K. The acute effects of transthoracic cryoablation on normal lung evaluated in a porcine model. *Ann Thorac Surg* 2005;79(1):318–322; discussion 322
- 38 Hinshaw JL, Littrup PJ, Durick N, et al. Optimizing the protocol for pulmonary cryoablation: a comparison of a dual- and triple-freeze protocol. *Cardiovasc Intervent Radiol* 2010;33(6):1180–1185
- 39 Permpongkosol S, Nicol TL, Link RE, et al. Differences in ablation size in porcine kidney, liver, and lung after cryoablation using the same ablation protocol. *AJR Am J Roentgenol* 2007;188(4):1028–1032
- 40 Niu L, Li J, Chen J, et al. Comparison of dual- and triple-freeze protocols for pulmonary cryoablation in a Tibet pig model. *Cryobiology* 2012;64(3):245–249